Widespread distribution of the BpfA-carrying bacteria involved in the bisphenol F degradation in Pseudomonadota and Actinomycetota

Changchang Wang[a,1], Mingliang Zhang[a,1], Yanni Huang[a], Qian Li[a], Junqiang Hu[a], Kaihua Pan[a], Qian Zhu[a], Wankui Jiang[b], Jiguo Qiu[a], Xin Yan[a*], Qing Hong[a*]

[a] Department of Microbiology, College of Life Sciences, Nanjing Agricultural University, Key Laboratory of Agricultural and Environmental Microbiology, Ministry of Agriculture and Rural Affairs, Nanjing 210095, China.

[b] State Key Laboratory of Materials-Oriented Chemical Engineering, College of Biotechnology and Pharmaceutical Engineering, Nanjing Tech University, Nanjing 211800, PR China.

[1] Contributed equally to this paper.

* Author for correspondence: Xin Yan and Qing Hong

E-mail address: yanxin@njau.edu.cn. and hongqing@njau.edu.cn.

Tel: +86-25-84396685, Fax: +86-25-84395326

ABSTRACT

The global use of bisphenol F (BPF) has led to widespread environmental contamination, posing significant threats to ecosystems and human health. However, the genes involved in BPF degradation remained unknown. In this study, a novel oxidase gene, *bpfA*, was obtained from strain *Microbacterium* sp. F2 through a four-step purification strategy. BpfA is classified as a member of the 4-phenol oxidizing (4PO) subfamily and contains a conserved FAD-binding domain (Asp152 and His393) as well as a Tyr-Tyr-Arg triad (Tyr93, Tyr474, Arg475). BpfA catalyzes the conversion of BPF to 4,4′-dihydroxydibenzophenone (DHBP) through a series of three consecutive reactions. In addition, BpfA exhibits catalytic activity towards 4-alkylphenols, such as vanillyl alcohol (VA), 4-n-propylguaiacol (4PG), and 4-(methoxymethyl)phenol (4MOP). BpfA homologs are widely distributed in the environment, particularly in soil. Bioinformatics-based taxonomic profiling revealed that BpfA homologs are widely distributed in metagenomes from cultivated land and forests, mainly belonging to Pseudomonadota and Actinomycetota. This study enhances our understanding of the microbial degradation mechanism of BPF, elucidates the catalytic function of the novel oxidase gene *bpfA* and its distribution pattern in the environment, and provides important insights into the evolutionary origin of BPF degradation genes and the targeted mining of environmental microbial resources.

KEYWORDS: Bisphenol F, Biodegradation, FAD-binding oxidoreductase BpfA, *Microbacterium* sp. F2, Distribution pattern.

Introduction

Bisphenols (BPs) are one of the important chemical raw materials for the synthesis of high-molecular-weight materials and are widely used in various consumer products, including bisphenol A (BPA), bisphenol F (BPF), bisphenol B (BPB), bisphenol S (BPS), and bisphenol AF (BPAF). However, toxicological studies have shown that BPA has endocrine-disrupting effects and may trigger a variety of health problems, such as cancer [1], reproductive disorders [2,3], and obesity [4,5]. As one of the main substitutes for BPA, the usage of BPF has increased year by year, and it has become a new, widely-present pollutant in water bodies [6]. BPF enters aquatic, soil, and atmospheric environments via industrial effluent discharge, plastic product degradation, and landfill leachate and has been widely detected globally [7,8]. BPF contamination in East Asian aquatic systems reaches notable levels, exceeding 1000 ng/L in rivers and seawater across Japan, Korea, and China; the highest concentration (2850 ng/L) was detected in Tokyo's Tamagawa River [9-11]. Moreover, the breast milk samples collected from 181 healthy women across various provinces and cities in China revealed an average BPF concentration of 0.107 μg/L [12]. This suggests that BPF, in addition to its widespread presence in the aquatic environment, may also pose risks to human health through bioaccumulation.

BPF has toxic effects on organisms. Exposure to 0.5 mM BPF during the embryonic stage of fruit flies reduced the number of neuroblasts and intermediate neural progenitor cells, leading to an imbalance in the neuron-to-glial cell ratio. This disrupted the proliferation of neural stem cells, resulting in neurodevelopmental

toxicity and abnormal larval behavior [13]. Through transcriptomic and metabolomic studies, it was found that exposure to 1.0 μM BPF upregulated the expression of pro-inflammatory cytokines (such as IL-17A and TNF-α) in human colonic epithelial cells (NCM460), while downregulating tight junction proteins (ZO-1 and CLDN1), thereby disrupting intestinal barrier function [14]. In addition, adult male zebrafish exposed to BPF concentrations of 500 nM and 2500 nM exhibited significant reductions in sperm count, decreased levels of serum testosterone (T), and increased levels of vitellogenin (VTG) in the liver, indicating that BPF has endocrine-disrupting effects on adult male zebrafish [15].

Several bacterial strains capable of growing with BPF have recently been identified, including *Pseudomonas* sp. HS-2 [16], *Pseudomonas* sp. ZH-FAD [17], *Sphingobium yanoikuyae* FM-2 [18], *Sphingobium yanoikuyae* TYF-1 [19], *Arthrobacter* sp. YC-RL1 [20], and *Microbacterium* sp. F2 [21]. The identification of similar intermediates in the BPF degradation process among strains from various genera has led to the proposal of a common catabolic pathway (Fig. S1). This pathway involves the initial hydroxylation of the BPF carbon bridge to form (4-hydroxyphenyl)methanol (BHPM), followed by dehydrogenation to produce 4,4´-dihydroxydibenzophenone (DHBP). Subsequently, the Baeyer-Villiger reaction occurs between the two phenolic rings to generate 4-hydroxybenzoic acid-4-hydroxyphenyl ester (HPHB), which is hydrolyzed into *p*-hydroxybenzoic acid (PHBA) and hydroquinone (HQ). These compounds are further degraded to provide carbon sources for the growth of the strains. Although several BPF-degrading bacterial strains have

been reported, the specific genes involved in the conserved BPF metabolic pathway remain unknown. Elucidating these BPF degradation genes is crucial for understanding the transformation and ultimate fate of BPF in the environment.

In the current study, a novel oxidase gene, *bpfA*, was identified in the previously isolated BPF-degrading strain *Microbacterium* sp. F2, which catalyzes the conversion of BPF to DHBP through three consecutive reactions. The classification of the *bpfA* gene and its distribution in various environments worldwide were analyzed. These results provide novel perspectives on the variety of BPF degradation genes across distinct microbial strains.

Materials and methods

Chemicals and media

Bisphenol F (BPF) and bisphenol E (BPE) were purchased from Sigma-Aldrich. Vanillyl alcohol (VA), 4,4′-dihydroxybenzophenone (DHBP), 4-*n*-propylguaiacol (4PG), 4-hydroxyphenyl 4-hydroxybenzoate (HPHB), 4-(Methoxymethyl) phenol (4MOP), *p*-hydroxybenzoic acid (PHBA), and 1,4-hydroquinone (HQ) were purchased from Shanghai Macklin Biochemical Technology Co., Ltd (Shanghai, China). The chromatography-grade methanol and acetic acid were purchased Nanjing Wanqing Chemical Glass Ware & Instrument Co., Ltd (Nanjing, China). BPF degradation experiments were performed in a mineral salts medium (MSM) with a pH of 7.0. The bacterial strains used in this study were cultured in lysogeny broth (LB) medium, also set at pH 7.0 [21]. The MMB medium was created by incorporating BPF at a concentration of 0.10 mM into the MSM. Other chemicals obtained from Beijing Vokai

106 Biotechnology Co., Ltd (Beijing, China) were of the available highest analytical grade.

107 Strains, plasmids, and cultural conditions

108 Details of the bacterial strains and plasmids utilized in this study are provided in
109 Supplementary Table S1. *Microbacterium* sp. F2 was cultured in LB broth or MMB at
110 30°C with shaking at 180 rpm, unless otherwise specified. *Escherichia coli* strains were
111 cultured in LB broth at 37°C and 200 rpm.

112 BPF degradation assay

113 Strain F2 was initially cultured in LB medium for 24 h, followed by centrifugation
114 at 4°C (5,000 × *g*, 5 min). The harvested cells were washed three times with sterile
115 MSM and subsequently resuspended in 2 mL of sterile MSM. The cells, adjusted to an
116 OD_{600} of 1.0, were then inoculated into MMB supplemented with 0.10 mM BPF and
117 incubated at 30°C. Aliquots (1 mL) were taken every 2 h and analyzed via high-
118 performance liquid chromatography (HPLC) to quantify BPF concentrations. A control
119 experiment was conducted using MSM without strain F2 under identical conditions. All
120 treatments were performed in triplicate.

121 To prepare BPF-induced cells, cells of strain F2 cultured in LB medium were
122 harvested, washed three times with sterile MSM, and then individually inoculated in
123 MSM containing 0.10 mM BPF. When half of the BPF was degraded, cells of strain F2
124 was collected, washed three times with sterile MSM, and resuspended in 2 mL of sterile
125 MSM to prepare BPF-induced cells. Subsequent BPF degradation experiments were
126 conducted as described above.

127 BPF-induced cell extracts were prepared by first collecting and washing the BPF-

128 induced cells of strain F2 twice with 20 mM Tris-HCl buffer (pH 8.0), followed by
129 resuspension in 15 mL of the same buffer. Subsequently, the cells were lysed in an ice
130 bath by ultrasonic processor (UH-650B, Auto Science) to obtain the BPF-induced cell
131 extracts. Centrifugation of the lysates was performed at 12,000 × g for 20 min at 4 °C.
132 For the BPF degradation experiments, a 3 mL reaction mixture containing 0.10 mM
133 BPF and 1 mL of cell lysate was prepared in a 20 mM Tris-HCl buffer (pH 8.0) at 30°C.
134 The reaction was terminated immediately by boiling for 5 min after completion.
135 Samples were collected every 10 min and analyzed by HPLC to measure the
136 concentration of BPF.

137 **Sequencing and analysis**

138 Genomic DNA from strain F2 was extracted using a commercial kit (TIANGEN
139 BIOTECH Co., LTD, Beijing, China). The genome of strain F2 (accession number:
140 JBNVBV000000000) was sequenced by Majorbio Biomedical Technology Co., Ltd
141 (Shanghai, China). Gene prediction and annotation were carried out using Glimmer
142 3.02 and RAST (Rapid Annotation Subsystem Technology) database
143 (https://rast.nmpdr.org/) [22].

144 **Purification of BpfA from the cell extract of strain F2**

145 The purification was conducted at 0-4°C using a 20 mM Tris-HCl buffer (pH 8.0).
146 The detailed protocol followed the methods previously reported [45]. The protein band
147 visualized on SDS-PAGE (Fig. S3, lane 6) was excised and subjected to peptide mass
148 spectrometry analysis. The resulting peptide fragments were matched against the
149 annotated genes from strain F2 to pinpoint sequences with high homology.

150 Subsequently, the resulting protein sequences underwent a BLASTP search against the
151 NCBI non-redundant protein (NR) database. Based on these analyses, the gene
152 encoding FAD-binding oxidoreductase, *bpfA*, was identified as a potential candidate for
153 catalyzing BPF and was selected for further protein expression and *in vitro* BPF
154 degradation assays.

155 **Bioinformatic Analysis**

156 A BLASTP search was conducted using the BpfA sequence (PV658135) from
157 *Microbacterium* sp. F2 as the query sequence, targeting all genomes within the NCBI
158 database to uncover BpfA homologues. The sequence similarity network (SSN) was
159 created utilizing the Enzyme Function Initiative Enzyme Similarity Tool (EFI-EST)
160 [23]. An all-by-all BLAST was performed on the sequences, and the SSN was
161 subsequently built based on an alignment score cutoff of 90. Visualization of the SSN
162 was accomplished with Cytoscape [24]. For the phylogenetic analysis of BpfA,
163 homologous sequences were retrieved from the NCBI NR database. These sequences
164 were aligned using the ClustalX [25], and the resultant alignment was transferred to
165 MEGA (version 11.0) [26] for further processing. The phylogenetic tree was
166 subsequently generated employing the neighbor-joining algorithm.

167 Previously, species-level genome bins (SGBs) were constructed from 3,304 soil
168 metagenomes, ensuring medium to high quality standards (with completeness
169 exceeding 50% and contamination below 10%). Further details are available at the
170 Global Soil MAGs Project website [27]. These SGBs were classified using GTDB-Tk
171 (version 1.6.0), and the BpfA protein was identified through Prodigal, with stringent

172 criteria (identity greater than 35%, e-value less than 1×10^{-5}, and subject coverage
173 over 95%) [28]. To explore the global distribution of BpfA, amino acid sequences from
174 the SGBs were obtained and analyzed via Diamond (v2.1.6). By integrating
175 classification data from SGBs and GTDB, a comprehensive analysis of BpfA species
176 distribution was accomplished [29]. Additionally, the classification of target genomes
177 as either isolated or uncultured (including metagenomic assembly genomes and single
178 amplified genomes) was determined by searching both GTDB and NCBI RefSeq [30].

179 Gene expression and purification of the recombinant enzyme

180 The primer pair $bpfA_{F2}$-F and $bpfA_{F2}$-R (Supporting Information Table S2) was
181 used to amplify the *bpfA* gene from strain F2. The amplified *bpfA* gene was cloned into
182 the NdeI/XhoI-digested pET29a(+) plasmid using the ClonExpress II one-step cloning
183 kit (Vazyme Biotech Co., Ltd., China), resulting in the recombinant plasmid pET-*bpfA*.
184 This plasmid was then introduced into *Escherichia coli* BL21(DE3) to create the
185 expression strain *E. coli* BL21(pET-*bpfA*). The strain *E. coli* BL21(pET-*bpfA*) was
186 inoculated into LB containing 50 mg/L kanamycin and cultured until the cell density
187 reached an OD_{600} of 0.5-0.6, at which point 0.2 mM IPTG was added to induce protein
188 expression for 12 h at 16°C. Cells were centrifuged and lysed using an ultrasonic
189 processor (UH-650B, Auto Science). The supernatant was obtained by centrifugation
190 at 4°C and then passed through a Ni-NTA column (Sangon, Shanghai, China). A series
191 concentrations of imidazole were used to elute the column and purify the recombinant
192 protein. The purified protein was then dialyzed overnight in Tris-HCl buffer (pH 8.0)
193 and analyzed by SDS-PAGE. A BCA kit from Vazyme Biotech Co., Ltd (Nanjing, China)

194 was used to determine the protein concentration.

195 The genes *eugO* from *Rhodococcus jostii* RHA1 (Q0SBK1), *vaO* from *Penicillium*
196 *simplicissimum* CBS 170.90 (P56216), and FAD-binding oxidoreductase gene *fbO*
197 from *Sphingobium* sp. W15 (PV658134) were synthesized from Nanjing Qingke
198 Biotechnology Co., Ltd (Nanjing, China). The protein expression and purification
199 methods for EUGO, VAO, and FAD-binding oxidoreductase were similar to those
200 described above.

201 **Enzyme activity assays**

202 Enzymatic assays for BpfA were performed at 30°C for 2 h in a 1 mL reaction
203 mixture containing 20 mM Tris-HCl buffer (pH 8.0), 0.10 mM BPF, and 3.0 μM BpfA.
204 The enzymatic reactions were terminated by boiling for 5min. Enzyme activity was
205 quantified as the amount of enzyme needed to convert 1 μmol of BPF per minute,
206 defined as one unit.

207 To determine the optimal reaction temperature, BpfA's activity was tested at
208 various temperatures, spanning from 20°C to 50°C in 5°C increments. The thermal
209 stability of BpfA was evaluated by subjecting the enzyme to different temperatures for
210 30 min, after which the residual activity was assessed under the specified assay
211 conditions. The non-heated enzyme was used as the control (100%). The optimal
212 reaction pH was determined using a variety of buffers: 20 mM Citrate-Phosphate buffer
213 (pH 4.0 to 6.0), 20 mM Tris-HCl buffer (pH 6.0 to 8.0), and 20 mM glycine-NaOH
214 buffer (pH 8.0 to 10.0). The pH stability of BpfA was examined by incubating the
215 enzyme at 4°C for 30 min in buffers with diverse pH, with residual activities

216 subsequently measured. Samples were collected prior to complete substrate
217 consumption. A reaction mixture devoid of the enzyme served as a negative control.
218 The activity of the reference enzyme was designated as 100%, and the relative activities
219 of each reaction were determined as a percentage relative to the reference.

220 To evaluate the substrate specificity of BpfA, the enzyme was tested with various
221 substrates (BPE, VA, 4PG, and 4MOP) at a concentration of 0.10 mM each, under the
222 reaction conditions described above. The activity assays for EUGO, VAO, and FBO
223 were similarly performed following the same procedures.

224 Site-directed mutagenesis

225 Mutations at specific sites within the *bpfA* gene were engineered via overlap
226 extension PCR. The primer pairs Y93A-F/R, Y474A-F/R, R475A-F/R, D152A-F/R,
227 and H393A-F/R were used to introduce the mutation sites (Table S2). The site-directed
228 mutagenesis amplification was carried out following the protocol provided with the
229 site-directed mutagenesis kit (Vazyme Biotech Co., Ltd., China). The resulting PCR
230 products were purified by gel extraction and ligated into pET-29a(+) vector, following
231 the previously described method. The activity assessment of the mutant proteins was
232 carried out using the previously detailed procedures.

233 Analytical methods

234 Enzyme assay samples were boiled for 5min and subsequently centrifuged at
235 12,000 × *g* for 5 min. The resulting supernatant was passed through a 0.2-mm-pore-size
236 membrane prior to further analysis of the products. The detection and quantification of
237 BPF and its metabolites in enzyme assay samples were performed using HPLC [21].

238 The identification of BpfA and its metabolites in enzyme assay samples was achieved
239 using mass spectrometry on an AB SCIEX Triple TOF 5600 [21].

240 Results and discussion

241 **Cloning and sequence analysis of *bpfA* gene.**

242 *Microbacterium* sp. F2 has been reported to use BPF as the sole carbon source for
243 growth, with BPF degradation being induced by BPF itself [21]. Furthermore, cell
244 extract from BPF-induced strain F2 completely degraded 0.10 mM BPF, regardless of
245 whether NADPH, NADH, and FAD were introduced (Fig. S2). Therefore, the gene
246 encoding the initial step of BPF degradation can be obtained from the cell extract of
247 strain F2 via protein purification techniques. A four-stage purification protocol was
248 utilized to refine the BPF-degrading enzyme from the cell extract of BPF-induced strain
249 F2. Initially, the specific activity in the cell extract from strain F2 was determined to be
250 0.37 U/mg protein. Following the four purification steps, the specific activity of the
251 final fraction rose to 14.74 U/mg, with a 24.15-fold increase in protein concentration
252 and a recovery rate of 4.76% (Table S3). Subsequent SDS-PAGE analysis of the final
253 fraction showed a single protein band (Fig. S3), which was excised and subjected to
254 peptide mass spectrometry analysis. The analysis yielded sequences of fifteen peptide
255 fragments, which were then matched against all annotated genes within strain F2
256 (JBNVBV000000000) (Table S4). Subsequently, all candidate genes predicted to
257 degrade BPF were annotated and experimentally validated. A FAD-binding
258 oxidoreductase-encoding gene, *orf1733* (ACQVDU_06965), demonstrated BPF-
259 degrading activity and was designated as *bpfA*, which was selected for further studies.

260 The *bpfA* gene (1,599 bp) encodes a 532-amino acid oxidase that shares 30%–55%
261 identity with FAD-binding oxidoreductases from various genera (Non-redundant
262 Protein Sequences Database). BpfA is classified within the flavoprotein oxidase
263 superfamily [31,32]. A sequence similarity network (SSN) analysis indicates that BpfA
264 is a member of the vanillyl alcohol oxidase (VAO) flavoprotein family (PF01565)
265 within this superfamily (Fig. 1A). BpfA shows 33% to 42% sequence identity with three
266 biochemically characterized oxidoreductases from *Rhodococcus jostii* RHA1 (vanillyl-
267 alcohol oxidase EUGO [Q0SBK1]; 41.14% identity) [33], *Penicillium simplicissimum*
268 CBS 170.90 (vanillyl-alcohol oxidase VAO [P56216]; 37.50% identity) [34], and
269 *Pseudomonas putida* NCIMB 9869 (*p*-cresol methylhydroxylase PCMH [P09788.3];
270 33.20% identity) [35]. These three enzymes are members of the VAO flavoprotein
271 family, which is characterized by a conserved FAD-binding domain [36] and a Tyr-Tyr-
272 Arg triad essential for substrate binding [37]. Additionally, the VAO flavoprotein family
273 (PF01565) is further divided into 11 subfamilies [37]. BpfA clusters with the reported
274 members of the 4-phenol oxidizing (4PO) subfamily, including EUGO (Q0SBK1),
275 PCMH (P09788.3), and VAO (P56216), suggesting that these proteins may have a
276 closer phylogenetic relationship and similar functions (Fig. 1B). BpfA and other
277 members of the 4PO subgroup, including EUGO, PCMH, and VAO, share five
278 conserved motifs (Fig. S4) [38]. The residues in the 4PO-motif-1 form a loop that
279 closely interacts with the FAD cofactor. Notably, one of the tyrosine residues (Tyr93),
280 which is essential for substrate deprotonation, is situated within this loop. The 4PO-
281 motif-5 also forms a loop that includes the other two residues, Tyr474 and Arg475,

involved in substrate deprotonation. Furthermore, the amino acids Asp152 and His393 are involved in forming a covalent bond with FAD, which is critical for the enzyme's redox properties. This covalent binding significantly enhances the redox potential of the enzyme [39], thereby accelerating the rate of FAD reduction by the substrate and, consequently, enhancing the overall reaction rate [39].

Functional identification of BpfA.

The purified BpfA protein displayed a pale yellow and showed a single band on SDS-PAGE, with an observed molecular mass of 59.9 kDa, which closely aligns with the theoretical molecular mass of 58.8 kDa (Fig. 2A). Purified BpfA was able to completely degrade 0.10 mM of BPF *in vitro* within 40 min. During the degradation of BpfA, four metabolites were identified (namely compound I, II, III, and IV) (Fig. 2B). The peak height of compound I (5.000 min) continuously decreased and completely disappeared at 40 min. After 20 min, compound II (3.998 min), compound III (2.708 min), and compound IV (3.703 min) appeared simultaneously with the degradation of compound I. However, compound II only appeared briefly before rapidly disappearing. Subsequently, compound III was gradually converted to compound IV and completely disappeared after 60 min. Ultimately, the peak height of compound IV continuously increased and remained unchanged. These compounds were identified by HPLC-MS as BPF (compound I, Fig. 2C), 4-[(4-hydroxyphenyl)methylene]cyclohexa-2,5-dien-1-one (HMC) (compound II, Fig. 2D), BHPM (compound III, Fig. 2E), and DHBP (compound IV, Fig. 2F). Additionally, we detected the production of 0.189 mM hydrogen peroxide (H_2O_2) during the degradation of 0.10 mM BPF by BpfA using the

304 H_2O_2 colorimetric method [40], with a ratio of approximately 1:2 (Fig. S5).

305 The identified metabolites led to the proposal of a BPF degradation pathway
306 mediated by BpfA (Fig. 2G). Initially, the phenolic -OH group of BPF is deprotonated
307 by two conserved tyrosine residues of BpfA (Y93 and Y474). The electron density is
308 then conducted through the aromatic ring, extruding a hydride ion (H^-) from the α-
309 position, which is accepted by the isoalloxazine ring of the oxidized flavin cofactor.
310 The resulting quinone methide intermediate (HMC) then acts as an electrophile,
311 undergoing nucleophilic addition with a water molecule catalyzed in the BpfA´s active
312 site, leading to the formation of the hydroxylated product (BHPM). Finally, BHPM
313 undergoes further dehydrogenation to generate DHBP. Meanwhile, FAD is reoxidized
314 by molecular oxygen, which is converted to H_2O_2. The initial deprotonation of the
315 phenolic hydroxyl group of the substrate is a crucial step in this mechanism, as it
316 facilitates the hydride transfer reaction by promoting the formation of the *para*-quinone
317 methide intermediate. The same effect has been observed in VAO and EUGO [41,42].

318 In this study, BpfA catalyze the sequential transformation of BPF into the quinone
319 methide intermediate HMC, BHPM, and DHBP (Fig. 2), which differs from the BPF
320 degradation pathway proposed in strain F2, in which BPF was metabolized into BHPM
321 and DHBP without the detection of the intermediate HMC [21]. According to the
322 previously reported VAO catalytic mechanism, the key product intermediate, quinone
323 methide, is transiently formed and allows for the rapid occurrence of several different
324 oxidation reactions [41,42]. We speculate that the quinone methide intermediate HMC
325 may be rapidly converted to BHPM in strain F2, and thus cannot be captured by HPLC.

326 In this study, purified BpfA is used to catalyze BPF *in vitro* and detected HMC through
327 multiple consecutive samplings. In short, The proposed BPF degradation pathway in
328 strain F2 was described at the cellular level but lacked genetic or enzymatic evidence.
329 However, this study elucidates the BPF degradation process at the enzymatic and
330 genetic levels and proposes a modified BPF metabolic pathway compared to that by
331 Wang et al. [21].

332 **BpfA and 4PO subfamily proteins**

333 To investigate the potential distribution of BpfA across different strains, we
334 searched the NCBI NR database for homologs with a coverage of no less than 95% and
335 at least 30% amino acid sequence identity. Consequently, 49 gene pairs belonging to
336 the 4PO subfamily were identified from three bacterial phyla, specifically from
337 Pseudomonadota (12), Actinomycetota (27), and Ascomycota (10) (Fig. 3A). The BpfA
338 homologs originate from soil, sediments, clinical specimens, wastewater, faeces,
339 pulping wastewater, oil-well water-associated microorganisms, indicating their
340 ubiquity in the environment. Phylogenetic tree analysis shows that BpfA, EUGO, VAO,
341 and PCMH are located on different branches, suggesting that they may not have evolved
342 directly from a single common ancestor but rather may have undergone different
343 branching events during the course of evolution. In order to determine if these BpfA
344 homologous genes were functional, we synthesized three genes from Ascomycota,
345 Actinomycetota and Pseudomonadota: EUGO (Q0SBK1; *Rhodococcus jostii* RHA1;
346 coverage 98%; identity 41.14%), VAO (P56216; *Penicillium simplicissimum* CBS
347 170.90; coverage 96%; identity 37.50%), and FAD-binding oxidoreductase FBO

348 (PV658134; *Sphingobium* sp. W15; coverage 97%; identity 39.46%), for the purpose
349 of expressing recombinant proteins in *E. coli*. Given that PCMH from *Pseudomonas*
350 *putida* NCIMB 9869 (Pseudomonadota) is a two-component protein with an $\alpha 2\beta 2$
351 structure, comprising an α-subunit (PchF) and a β-subunit (PchC) to function [35], and
352 considering that the reported EUGO and VAO are both single-component proteins, this
353 study did not consider synthesizing PCMH for subsequent functional validation.

354 In the absence of FAD, VAO, EUGO, and FBO exhibited weak activity against
355 BPF, with the specific activity of BpfA being 2452, 2907, and 3672 times higher than
356 that of VAO, EUGO, and FBO, respectively (Fig. 3B). In the presence of FAD, the
357 specific activity of BpfA was 2381, 2809, and 2104 times higher than that of VAO,
358 EUGO, and FBO, respectively (Fig. 3B). There was no significant difference in the
359 catalytic activity of VAO and EUGO against BPF, regardless of the presence or absence
360 of FAD. Compared with VAO and EUGO, the addition of FAD significantly enhanced
361 the catalytic activity of FBO against BPF. Further analysis revealed that FBO (D to G
362 mutation) each had only one amino acid residue involved in FAD binding altered (Fig.
363 3A). Therefore, the addition of FAD was required for FBO to exhibit higher catalytic
364 activity. The above results indicate that members of the 4PO subfamily proteins exhibit
365 catalytic activity against BPF.

366 **Biochemical characterization of BpfA.**

367 The specific BpfA activity was 14.71 U mg^{-1} protein for BPF (Fig. 3B). The highest
368 BPF activity was observed at a temperature of 30°C and a pH of 8.0 (Fig. S6). When
369 the enzyme was exposed to 40°C for 30 min, it maintained over 80% of its initial

activity. In contrast, incubation at 45°C for the same duration resulted in significant instability, with the enzyme retaining only 30% of its initial activity (Fig. S6A). BpfA exhibits high activity at a pH of 8.0, with its activity dropping below 20% at pH less than 5.0. When stored for 30 min at pH ranging from 7.0 to 10.0, its activity remains at 70% (Fig. S6B).

BpfA exhibits catalytic activity against other *para*-substituted phenolic compounds, including vanillyl alcohol (VA), 4-n-propylguaiacol (4PG), and 4-(methoxymethyl)phenol (4MOP) (Fig. 3C). The specific activity of BpfA against BPF is 249, 2.09, and 210 times higher than that against VA, 4PG, and 4MOP, respectively. However, BpfA does not exhibit catalytic activity against bisphenol E (BPE), which has a structure similar to BPF (Fig. S7), indicating that the two active hydrogen atoms on the α-position carbon of *para*-substituted phenolic compounds are crucial for BpfA to function.

Moreover, the Tyr-Tyr-Arg triad and conserved FAD-binding domain (Y93, Y474, R475, D152, and H393) of BpfA was replaced by alanine, resulting in five variants ($BpfA^{Y93A}$, $BpfA^{Y474A}$, $BpfA^{R475A}$, $BpfA^{D152A}$, and $BpfA^{H393A}$) (Fig. S8). Among the five mutants, only the purified $BpfA^{Y474A}$ and $BpfA^{H393A}$ exhibited the same pale yellow as the wild-type BpfA (Fig. S8A). $BpfA^{Y474A}$ and $BpfA^{H393A}$ retained 6.6% and 71.1% of their activity against BPF, respectively, while the other mutants completely lost their catalytic activity against BPF (Fig. S8B). This indirectly highlights the significance of the Tyr-Tyr-Arg triad for BpfA´s functionality and also indicates that Asp152 plays a more crucial role than His393 in forming a covalent bond with FAD. This also explains

392 why FBO require the addition of FAD to exhibit stronger catalytic activity. The results
393 confirm that BpfA belongs to the 4PO subfamily, featuring the Tyr-Tyr-Arg triad and a
394 conserved FAD-binding domain.

395 **Global survey on the environmental distributions of *bpfA* gene.**

396 Considering that BpfA homologs are predominantly derived from soil microbes
397 (Fig. 3), we conducted a mapping of BpfA reference sequences onto the species-level
398 microbial genomes present in GTDB and SGBs, aiming to investigate the diversity of
399 BpfA throughout the microbial tree of life. Among 153,143 microbial species across 12
400 phyla, BpfA homologs were identified in 1.08% (1652 genomes) of the species. The
401 study revealed that 67.37% of the microbial species potentially harboring the *bpfA* gene
402 remain uncultured (Fig. S9). BpfA was frequently found among Pseudomonadota
403 (70.04%) and Actinomycetota (20.46%) in the bacterial phyla. However, BpfA was not
404 observed in the archaea phyla (Fig. 4A). Notably, the genera *Paraburkholderia*,
405 *Novosphingobium*, and *Sphingobium* emerged as major bacterial taxa containing BpfA,
406 whereas only a few strains within the genus *Microbacterium* harbor this enzyme (Fig.
407 4B). Combining previously reported BPF-degrading strains, we can infer that bacteria
408 carrying the BpfA and involved in BPF degradation are widely distributed across
409 Pseudomonadota and Actinomycetota. These results expand our knowledge of the
410 variety of bacteria carrying BpfA that participate in BPF biodegradation. Grasping the
411 diversity and distribution of these bacteria is essential for elucidating their ecological
412 importance and potential applications.

413 The functional spectrum of BpfA was delineated by mapping its reference

414 sequences with 3304 metagenomic samples from a wide range of global environments.
415 The study found that BpfA exhibits distinct regional distribution patterns (Fig. 4C).
416 Geographically, BpfA homologs is primarily distributed across Asia, North America,
417 and Europe. These homologs are particularly abundant in environments such as
418 cultivated land and forests, which produce large amounts of lignocellulosic waste (such
419 as wheat straw, corn stover, and trees) annually. These wastes are degraded by soil
420 microbes to produce 4-alkylphenols. The biodegradation of 4-alkylphenols in cultivated
421 land and forests may be significantly influenced by bacteria carrying BpfA. In contrast,
422 in environments with less vegetation and tree cover, such as bare land, shrubland, and
423 tundra, the abundance of BpfA homologs is much lower.

424 Theoretically, the gene encoding BpfA-an enzyme capable of efficiently degrading
425 BPF-may have existed in pre-industrial gene pools. In other words, the ancestral gene
426 of *bpfA* could have been present in nature before humans synthesized BPF. This broad
427 substrate specificity indicates that BpfA has evolved the capability to degrade a range
428 of structurally similar compounds, likely stemming from its ancestral enzyme's role in
429 degrading naturally occurring 4-alkylphenols compounds. BpfA's subsequent evolution
430 to degrade the synthetic compound BPF supports the hypothesis that its progenitor
431 existed pre-industrially to metabolize phenolic intermediates. However, it is also
432 possible that there exists a relatively short evolutionary path from an unknown extant
433 gene to the *bpfA* gene identified in current biodegradation pathways. It has been
434 proposed that a novel sequence for an enzyme targeting a synthetic compound (e.g.,
435 BPF) could evolve via the activation of an unused alternative open reading frame within

436 a pre-existing repetitive coding sequence [43]. However, it is important to note that the
437 similarity between BpfA and members of enzyme superfamilies that catalyze other
438 reactions typically does not provide specific insights into the adaptation process to
439 xenobiotic compounds. The sequence similarity between BpfA and other proteins in
440 phylogenetic families is generally less than 55% (Fig. 3), suggesting that the divergence
441 of BpfA from these enzymes likely occurred much earlier than a century ago. Thus, its
442 evolutionary process cannot be simply attributed to the introduction of industrial
443 chemicals such as BPF into the environment. If BpfA and other key enzymes in
444 metabolic pathways had undergone recent mutations, closely related sequences with
445 only a few mutations differing from the current BpfA enzyme should be present in
446 nature. However, to date, no such primitive BpfA enzyme has been found in the NCBI
447 database. This suggests that BpfA may not have evolved through recent mutation events
448 but rather through more complex evolutionary processes, such as gene mutation or
449 recombination, to acquire its ability to degrade BPF.

450 Nevertheless, BpfA not only exhibits high degradative activity against BPF but
451 also shows some activity towards 4-alkylphenols, which are products of lignocellulosic
452 biomass reductive catalytic fractionation (RCF) [44], such as vanillyl alcohol (VA), 4-
453 n-propylguaiacol (4PG), and 4-(methoxymethyl)phenol (4MOP). This broad substrate
454 specificity of BpfA indicates that it has retained the metabolic function for natural
455 phenolic compounds while evolving the capability to degrade BPF. It is precisely this
456 enzymatic promiscuity of BpfA that makes it a potential biocatalyst for converting 4-
457 alkylphenol compounds into valuable phenolic monomers.

Conclusions

Given the widespread use of BPF, the residues of BPF in the environment cannot be overlooked. However, the metabolic degradation process of BPF by microorganisms is currently poorly understood. In this study, we cloned and identified a novel oxidase gene, *bpfA*, from *Microbacterium* sp. F2, which is responsible for catalyzing BPF into DHBP in a series of reactions. BpfA not only exhibits high degradation activity against BPF but also shows certain activity against 4-alkylphenol compounds such as VA, 4PG, and 4MOP. According to our survey of BpfA in the Global Soil MAGs Project metagenome database, BpfA homologs are widely distributed in the environment, especially in the metagenomes of cultivated land and forests, mainly belonging to Pseudomonadota and Actinomycetota. This study deepens our understanding of the microbial degradation mechanism of BPF, revealing the catalytic function of the novel oxidase gene *bpfA* and its distribution pattern in the environment.

Author contributions

C.W., M.Z. and Q.H. conceived and developed the study. C.W., M.Z., Y.H. and Q.H. gathered the data and conducted the analyses. C.W., M.Z. and Q.H. led the writing of the manuscript. Q.L., J.H., K.P., Q.Z. and W.J. contributed critically to the analyses and writing. J.Q., X.Y. and Q.H. directed the study and critically revised the manuscript for important intellectual content. All authors edited the manuscript and approved the final version.

Conflict of Interest

No conflict of interest exits in the submission of this manuscript, and manuscript is approved by all authors for publication.

Acknowledgements

This work was supported by the National Key R&D Program of China (2022YFA0912500), the National Natural Science Foundation of China (32170125 and 32400085), and the Postdoctoral Fellowship Program of CPSF (GZC20231127).

References

1. Lin J, Deng L, Sun M, et al. An *in vitro* investigation of endocrine disrupting potentials of ten bisphenol analogues. Steroids. 2021; 169: 108826.
2. Jiang X, Yin L, Zhang N, et al. Bisphenol A induced male germ cell apoptosis via IFN*β*-XAF1-XIAP pathway in adult mice. Toxicol Appl Pharmacol. 2018; 355: 247-256.
3. Pellerin E, Caneparo C, Chabaud S, Bolduc S, Pelletier M. Endocrine-disrupting effects of bisphenols on urological cancers. Environ Res. 2021; 195: 110485.
4. Kawa IA, Akbar Masood, Fatima Q, et al. Endocrine disrupting chemical Bisphenol A and its potential effects on female health. Diabetes Metab Syndr. 2021; 15(3) :803-811.
5. Rahman MS, Pang WK, Ryu DY, Park YJ, Ryu BY, Pang MG. Multigenerational impacts of gestational bisphenol A exposure on the sperm function and fertility of male mice. J Hazard Mater. 2021; 416: 125791.
6. Chen D, Kannan K, Tan H, et al. Bisphenol analogues other than BPA: environmental occurrence, human exposure, and toxicity-A Review. Environ Sci Technol. 2016;50(11):5438-5453.
7. Yang Y, Lu L, Zhang J, Yang Y, Wu Y, Shao B. Simultaneous determination of seven bisphenols in environmental water and solid samples by liquid chromatography-electrospray tandem mass spectrometry. J Chromatogr A. 2014; 1328: 26-34.
8. Fromme H, Küchler T, Otto T, Pilz K, Müller J, Wenzel A. Occurrence of phthalates and bisphenol A and F in the environment. Water Res. 2002; 36(6): 1429-1438.
9. Yamazaki E, Yamashita N, Taniyasu S, et al. Bisphenol A and other bisphenol analogues including BPS and BPF in surface water samples from Japan, China, Korea and India. Ecotoxicol Environ Saf. 2015; 122: 565-572.
10. Yan Z, Liu Y, Yan K, et al. Bisphenol analogues in surface water and sediment from the shallow Chinese freshwater lakes: Occurrence, distribution, source apportionment, and ecological and human health risk. Chemosphere. 2017; 184: 318-328.
11. Zhao B, Tan X, Xue M, et al. Pollution status and distribution characteristics of bisphenols in rivers of Guangyuan city. Environmental Monitoring and Forewarning. 2023; 15(6): 17-23.
12. Niu Y, Wang B, Yang R, et al. Bisphenol Analogues and Their Chlorinated Derivatives in

Breast Milk in China: Occurrence and Exposure Assessment. J Agric Food Chem. 2021; 69(4): 1391-1397.

13. Wang B, Yang Z, Zhang K, et al. Embryonic BPF exposure induces neurodevelopmental and neurobehavioral toxicity by affecting neural stem cell proliferation in *Drosophila*. Environ Pollut. 2025; 369: 125844.

14. Liu Y, Tang W, Ao J, Zhang J, Feng L. Transcriptomics integrated with metabolomics reveals the effect of Bisphenol F (BPF) exposure on intestinal inflammation. Sci Total Environ. 2022; 816: 151644.

15. Wu W, Su Z, Luo C, et al. Bisphenol F (BPF) exposure impairs sperm quality and offspring development in male zebrafish. Toxicol Appl Pharmacol. 2025; 496: 117245.

16. Wei H, Lu H, Zhou J, Wang J, Zhang Q, Zhou Y. Research on the characteristics of bisphenol F degradation and denitrification by *Pseudomonas* sp. HS-2. Ind Water Treatment. 2018; 38(01): 52-56.

17. Lu H, Li JY, Ma LC, et al. Simultaneous removal of bisphenol F and nitrate by a novel isolated strain *Pseudomonas* sp. ZH-FAD. AIP Conf Proc. 2022; 2474: 020003.

18. Inoue D, Hara S, Kashihara M, et al. Degradation of Bis(4-Hydroxyphenyl)methane (bisphenol F) by *Sphingobium yanoikuyae* strain FM-2 isolated from river water. Appl Environ Microbiol. 2008; 74(2): 352-358.

19. Toyama T, Sato Y, Inoue D, et al. Biodegradation of bisphenol A and bisphenol F in the rhizosphere sediment of *Phragmites australis*. J Biosci Bioeng. 2009; 108(2): 147-150.

20. Ren L, Jia Y, Ruth N, et al. Biotransformations of bisphenols mediated by a novel Arthrobacter sp. strain YC-RL1. Appl Microbiol Biotechnol. 2016; 100(4): 1967-1976.

21. Wang C, Li Q, Pan K, et al. Complete mineralization of bisphenol F by a newly isolated *Microbacterium* sp. F2 eliminates its toxicity to sensitive organisms. Int Biodeter Biodegr. 2025; 203: 106109.

22. Brettin T, Davis JJ, Disz T, et al. RASTtk: a modular and extensible implementation of the RAST algorithm for building custom annotation pipelines and annotating batches of genomes. Sci Rep. 2015; 5: 8365.

23. Oberg N, Zallot R, Gerlt JA. EFI-EST, EFI-GNT, and EFI-CGFP: Enzyme Function Initiative (EFI) Web Resource for Genomic Enzymology Tools. J Mol Biol. 2023; 435(14):

168018.
24. Doncheva NT, Morris JH, Holze H, et al. Cytoscape stringApp 2.0: Analysis and Visualization of Heterogeneous Biological Networks. J Proteome Res. 2023; 22(2): 637-646.
25. Kohli DK, Bachhawat AK. CLOURE: Clustal Output Reformatter, a program for reformatting ClustalX/ClustalW outputs for SNP analysis and molecular systematics. Nucleic Acids Res. 2003; 31(13): 3501-3502.
26. Tamura K, Stecher G, Kumar S. MEGA11: Molecular Evolutionary Genetics Analysis Version 11. Mol Biol Evol. 2021; 38(7): 3022-3027.
27. Ma B, Lu C, Wang Y, et al. A genomic catalogue of soil microbiomes boosts mining of biodiversity and genetic resources. Nat Commun. 2023; 14(1): 7318.
28. Hyatt D, Chen GL, Locascio PF, Land ML, Larimer FW, Hauser LJ. Prodigal: prokaryotic gene recognition and translation initiation site identification. BMC Bioinformatics. 2010; 11: 119.
29. Parks DH, Chuvochina M, Rinke C, Mussig AJ, Chaumeil PA, Hugenholtz P. GTDB: an ongoing census of bacterial and archaeal diversity through a phylogenetically consistent, rank normalized and complete genome-based taxonomy. Nucleic Acids Res. 2022; 50(D1): D785-D794.
30. Tang ST, Song XW, Chen J, et al. Widespread Distribution of the *arsO* gene confers bacterial resistance to environmental antimony. Environ Sci Technol. 2023; 57(39): 14579-14588.
31. Dijkman WP, de Gonzalo G, Mattevi A, Fraaije MW. Flavoprotein oxidases: classification and applications. Appl Microbiol Biotechnol. 2013; 97(12): 5177-5188.
32. Copp JN, Anderson DW, Akiva E, Babbitt PC, Tokuriki N. Exploring the sequence, function, and evolutionary space of protein superfamilies using sequence similarity networks and phylogenetic reconstructions. Methods Enzymol. 2019; 620: 315-347.
33. Guo Y, Alvigini L, Trajkovic M, et al. Structure- and computational-aided engineering of an oxidase to produce isoeugenol from a lignin-derived compound. Nat Commun. 2022; 13(1): 7195.
34. Ewing TA, Nguyen QT, Allan RC, et al. Two tyrosine residues, Tyr-108 and Tyr-503, are

responsible for the deprotonation of phenolic substrates in vanillyl-alcohol oxidase. J Biol Chem. 2017; 292(35): 14668-14679.

35. Kim J, Fuller JH, Cecchini G, McIntire WS. Cloning, sequencing, and expression of the structural genes for the cytochrome and flavoprotein subunits of *p*-cresol methylhydroxylase from two strains of *Pseudomonas putida*. J Bacteriol. 1994;176(20):6349-6361.

36. Leferink NG, Heuts DP, Fraaije MW, van Berkel WJ. The growing VAO flavoprotein family. Arch Biochem Biophys. 2008; 474(2): 292-301.

37. Ewing TA, Fraaije MW, Mattevi A, van Berkel WJH. The VAO/PCMH flavoprotein family. Arch Biochem Biophys. 2017; 632: 104-117.

38. Gygli G, de Vries RP, van Berkel WJH. On the origin of vanillyl alcohol oxidases. Fungal Genet Biol. 2018; 116: 24-32.

39. Fraaije MW, van den Heuvel RH, van Berkel WJ, Mattevi A. Covalent flavinylation is essential for efficient redox catalysis in vanillyl-alcohol oxidase. J Biol Chem. 1999; 274(50): 35514-35520.

40. Sambrook, J.; Fritsch, E. F.; Maniatis, T. Molecular cloning: a laboratory manual (No. Ed. 2), Cold spring harbor laboratory press. 1989.

41. Fraaije MW, van Berkel WJ. Catalytic mechanism of the oxidative demethylation of 4-(methoxymethyl)phenol by vanillyl-alcohol oxidase. Evidence for formation of a *p*-quinone methide intermediate. J Biol Chem. 1997; 272(29): 18111-18116.

42. Nguyen QT, de Gonzalo G, Binda C, Rioz-Martínez A, Mattevi A, Fraaije MW. Biocatalytic Properties and Structural Analysis of Eugenol Oxidase from *Rhodococcus jostii* RHA1: A Versatile Oxidative Biocatalyst. Chembiochem. 2016; 17(14): 1359-1366.

43. Ohno S. Birth of a unique enzyme from an alternative reading frame of the preexisted, internally repetitious coding sequence. Proc Natl Acad Sci U S A. 1984; 81(8): 2421-2425.

44. Renders T, Van den Bossche G, Vangeel T, Van Aelst K, Sels B. Reductive catalytic fractionation: state of the art of the lignin-first biorefinery. Curr Opin Biotechnol. 2019; 56: 193-201.

45. Zhang M, Bai X, Li Q, et al. Functional analysis, diversity, and distribution of carbendazim hydrolases MheI and CbmA, responsible for the initial step in carbendazim degradation. Environ Microbiol. 2022; 24(10): 4803-4817.

604 **Figure Legends**

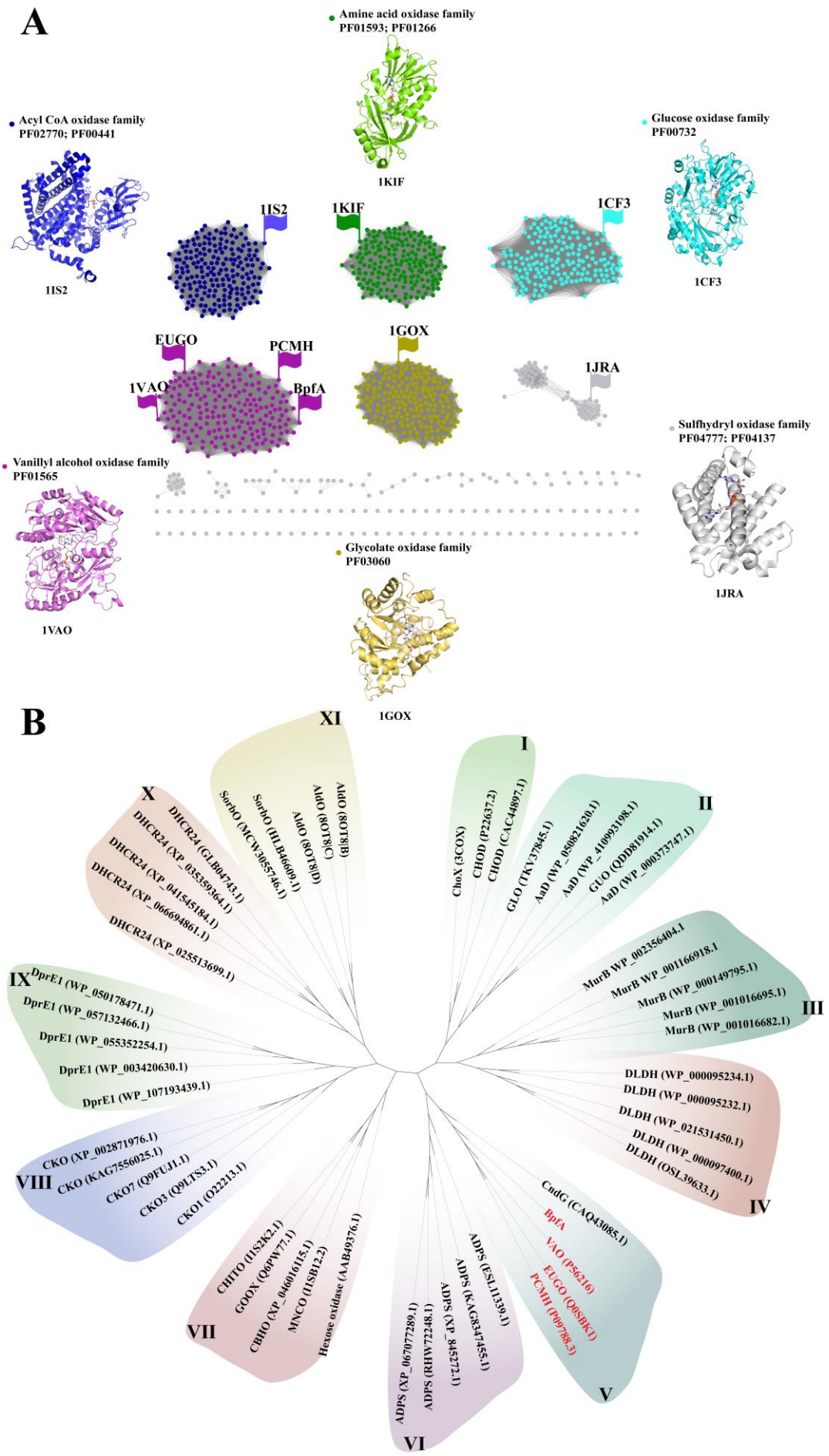
A
Amine acid oxidase family
PF01593; PF01266
1KIF
Acyl CoA oxidase family
PF02770; PF00441
1IS2
Glucose oxidase family
PF00732
1CF3
1IS2
1KIF
1CF3
EUGO
PCMH
1VAO
BpfA
1GOX
1JRA
Sulfhydryl oxidase family
PF04777; PF04137
Vanillyl alcohol oxidase family
PF01565
1VAO
Glycolate oxidase family
PF03060
1GOX
1JRA
B
XI
AldO (8OT8|B)
AldO (8OT8|C)
AldO (8OT8|D)
SorbO (HLB46609.1)
SorbO (MCW3055746.1)
X
DHCR24 (GLB04743.1)
DHCR24 (XP_035359364.1)
DHCR24 (XP_041545184.1)
DHCR24 (XP_066694861.1)
DHCR24 (XP_025513699.1)
I
ChoX (3COX)
CHOD (P22637.2)
CHOD (CAC44897.1)
II
GLO (TKV37845.1)
AaD (WP_050821620.1)
AaD (WP_410993198.1)
GUO (QDD81914.1)
AaD (WP_000373747.1)
III
MurB WP_002356404.1
MurB WP_001166918.1
MurB (WP_000149795.1)
MurB (WP_001016695.1)
MurB (WP_001016682.1)
IX
DprE1 (WP_050178471.1)
DprE1 (WP_057132466.1)
DprE1 (WP_055352254.1)
DprE1 (WP_003420630.1)
DprE1 (WP_107193439.1)
IV
DLDH (WP_000095234.1)
DLDH (WP_000095232.1)
DLDH (WP_021531450.1)
DLDH (WP_000097400.1)
DLDH (OSL39633.1)
VIII
CKO (XP_002871976.1)
CKO (KAG7556025.1)
CKO7 (Q9FUJ1.1)
CKO3 (Q9LTS3.1)
CKO1 (O22213.1)
V
CndG (CAQ43085.1)
BpfA
VAO (P56216)
EUGO (Q0SBK1)
PCMH (P09788.2)
VII
CHITO (I1S2K2.1)
GOOX (Q6PW77.1)
CBHO (XP_046016115.1)
MNCO (I1SB12.2)
Hexose oxidase (AAB49376.1)
VI
ADPS (XP_067077289.1)
ADPS (RHW72248.1)
ADPS (XP_845272.1)
ADPS (KAG8347455.1)
ADPS (ESL11339.1)

606 **Fig. 1.** (A) Sequence similarity network (SSN) for representative flavoprotein oxidase
607 superfamily in the NCBI Non-redundant Protein Sequences Database. Each item is
608 arranged in the following order: protein name and accession number. The around are
609 shown the structures of representative members of the different flavin-dependent
610 oxidases with the FAD or FMN cofactor highlighted in gold. (B) Phylogenetic analysis
611 of BpfA with the sequences of other members of the VAO flavoprotein family. I:
612 cholesterol oxidases subfamily; II: aldonolactone oxidoreductases subfamily; III:
613 MurBs subfamily; IV: α-Hydroxy acid dehydrogenases subfamily; V: 4-phenol
614 oxidizing subfamily; VI: alkyl-dihydroxyacetone phosphate synthases subfamily; VII:
615 BBE-like subfamily; VIII: cytokinin dehydrogenases subfamily; IX: DprE1s subfamily;
616 X: sterol reductases subfamily; XI: alditol oxidases subfamily.
617
618

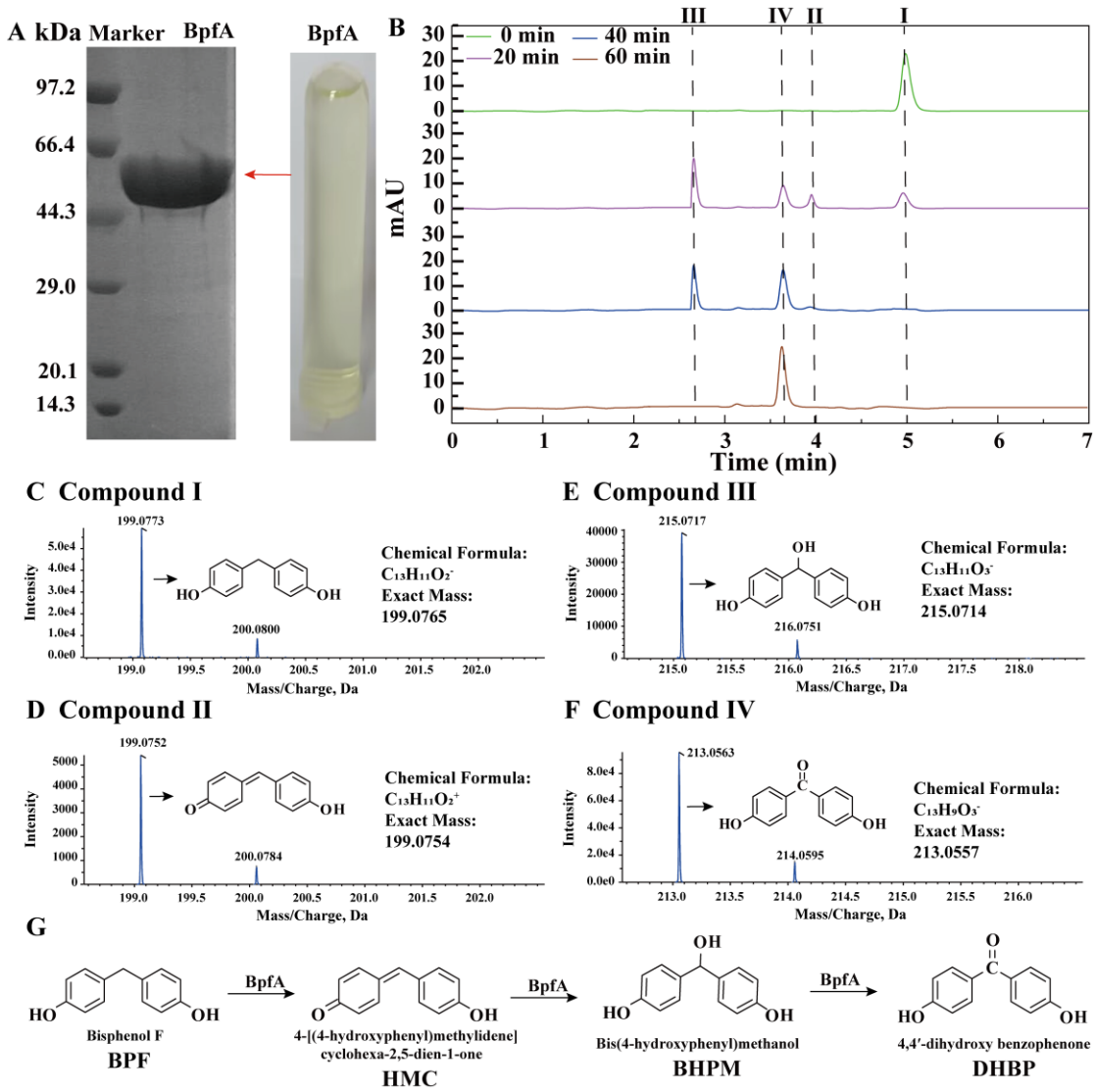

Fig. 2. HPLC-MS analysis of BPF products treated with BpfA. (A) SDS-PAGE analysis of the purified BpfA. (B) HPLC analysis of metabolites that appeared during the conversion of BPF by purified BpfA. (C) HPLC-MS analysis of compound I (*m/z* 199.0773 $[M-H]^-$), which was identified as BPF. (D) HPLC-MS analysis of compound II (*m/z* 199.0752 $[M+H]^+$), which was identified as HMC. (E) HPLC-MS analysis of compound III (*m/z* 215.0717 $[M-H]^-$), which was identified as BHPM. (F) HPLC-MS analysis of compound IV (*m/z* 213.0563 $[M-H]^-$), which was identified as DHBP. (G) The proposed metabolic pathway of BPF degradation by BpfA. BPF: bisphenol F; HMC: 4-[(4-hydroxyphenyl)methylidene]cyclohexa-2,5-dien-1-one; BHPM: bis (4-

629 hydroxyphenyl) methanol; DHBP: 4,4´-dihydroxybenzophenone.

630

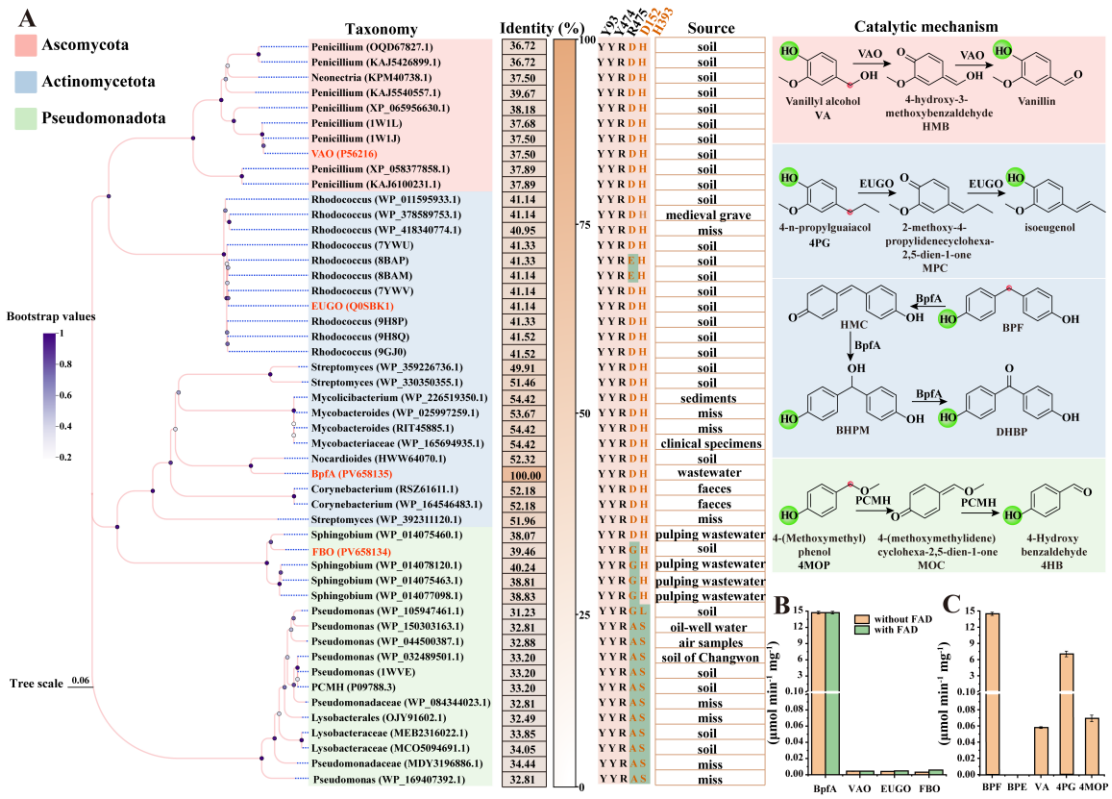

Fig. 3. Bioinformatic and functional analyzes of the 4-phenol oxidizing (4PO) subfamily proteins. (A) Phylogenetic tree of BpfA. The identity of BpfA homologous sequences is indicated on the right side of the phylogenetic tree. The three conserved key amino acid residues (black) and two conserved FAD-binding sites (orange) for each sequence are shown on the right side, and their positions in BpfA are indicated on the top of the columns. The residues with a green background are mutated residues, differing from the conserved residues marked with a pink background. The sources of strains containing BpfA homologous sequences are listed on the right side of the conserved amino acid sequences. On the far right side of the phylogenetic tree detail the catalytic mechanisms of VAO, BpfA, EUGO, and PCMH for their respective substrates. Green spheres represent invariant residues; red spheres indicate the catalytic sites of the reactions. (B) Assessment of the BPF activity of BpfA, VAO, EUGO, and

644 FBO. The data represent the mean values of two replicates using independent enzyme
645 preparation. (C) Assessment of the BPF, BPE, VA, 4PG, and 4MOP enzyme activity of
646 BpfA. The data represent the mean values of two replicates using independent enzyme
647 preparation.
648

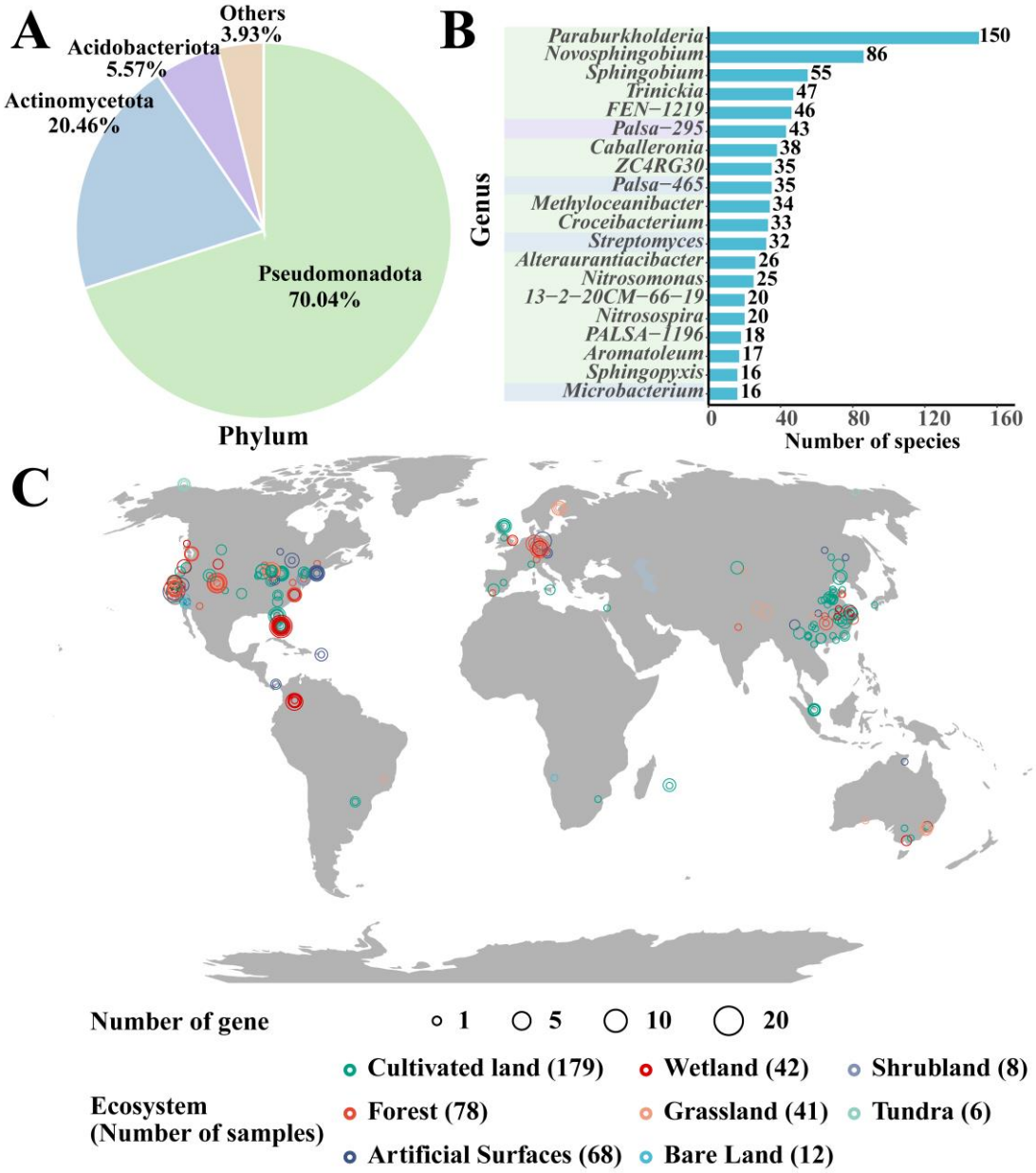

Fig. 4. Microbial classification and distribution pattern of the BpfA in global environments. (A) The number of species that mapped the BpfA across phyla in the domain of bacteria and archaea. (B) The number of species that mapped the BpfA across genera in the domain of bacteria and archaea. (C) Geographic and abundance distribution of the BpfA-harboring bacteria.